Ma *et al. Biochar* (2026) 8:51
https://doi.org/10.1007/s42773-025-00553-0

Biochar

ORIGINAL RESEARCH

Open Access

Fourteen-year field evidence reveals superior co-benefits of biochar in immobilizing heavy metals and sequestering carbon

Mengmeng Ma[1], Yunqian Zhang[1], Qiwen Ma[1], Zhibo Wang[1], Zhangliu Du[2], Yalan Chen[1*], Qun Gao[1], Fei Wang[1], Bo Gao[3] and Ke Sun[1*]

Abstract

Heavy metal contamination in global agricultural soils has posed severe ecological and health risks. However, little is known about the long-term effects of soil management on the bioavailable concentration and the speciation of heavy metals, especially via physicochemical and microbial processes. Utilizing a 14-year field trial, we showed that high-dosage biochar (HBC) effectively reduced heavy metal bioavailability by 2–91%, outperforming low-dosage biochar (LBC) and straw amendments. Both HBC and LBC drove residual Cd, Zn, and Pb toward reducible fractions, whereas straw exhibited no significant impact. Partial least squares-structural equation modeling and variance partitioning analysis indicated that the concentration and speciation of metals were co-regulated by physicochemical and microbial properties, with microbial attributes dominating bioavailability (30% variance) and physicochemical governing speciation (12%). Specifically, biochar reduced bioavailability by increasing the cation exchange capacity (CEC), soil organic carbon (SOC), and free iron oxides, coupled with enriching Entomophthoromycota and Nitrospirae while suppressing Bacteroidetes and Verrucomicrobia. Conversely, straw increased bioavailability by decreasing CEC but enhancing enzyme activity alongside Bacteroidetes or Verrucomicrobia. For metal speciation, biochar drove the transformation of speciation by enhancing SOC, aromatic compound levels, and Zoopagomycota, but suppressing Ascomycota and Latescibacteria. By evaluating the coupling index of heavy metal immobilization and carbon sequestration, we showed that HBC had a higher score (0.703) than LBC (0.361) and straw (0.396). This indicated that HBC can more effectively immobilize heavy metals than LBC and straw, and achieve extra benefits in promoting carbon sequestration. Our results provided insights into adjusting soil management practices to achieve soil multi ecosystem functions and improve agricultural sustainability.

Highlights

- Coupling index shows HBC can synergistically immobilize heavy metal and sequester C.
- HBC reduced heavy metal bioavailability and drove residual toward reducible fractions.
- Heavy metal bioavailability was dominated by Entomophthoromycota and Bacteroidetes.
- Heavy metal speciation was governed by SOC content and aromaticity.

Keywords Biochar, Heavy metal immobilization, Bioavailability, Speciation, Carbon sequestration

---

*Correspondence:
Yalan Chen
chenyalan@bnu.edu.cn
Ke Sun
sunke@bnu.edu.cn
Full list of author information is available at the end of the article

Graphical Abstract

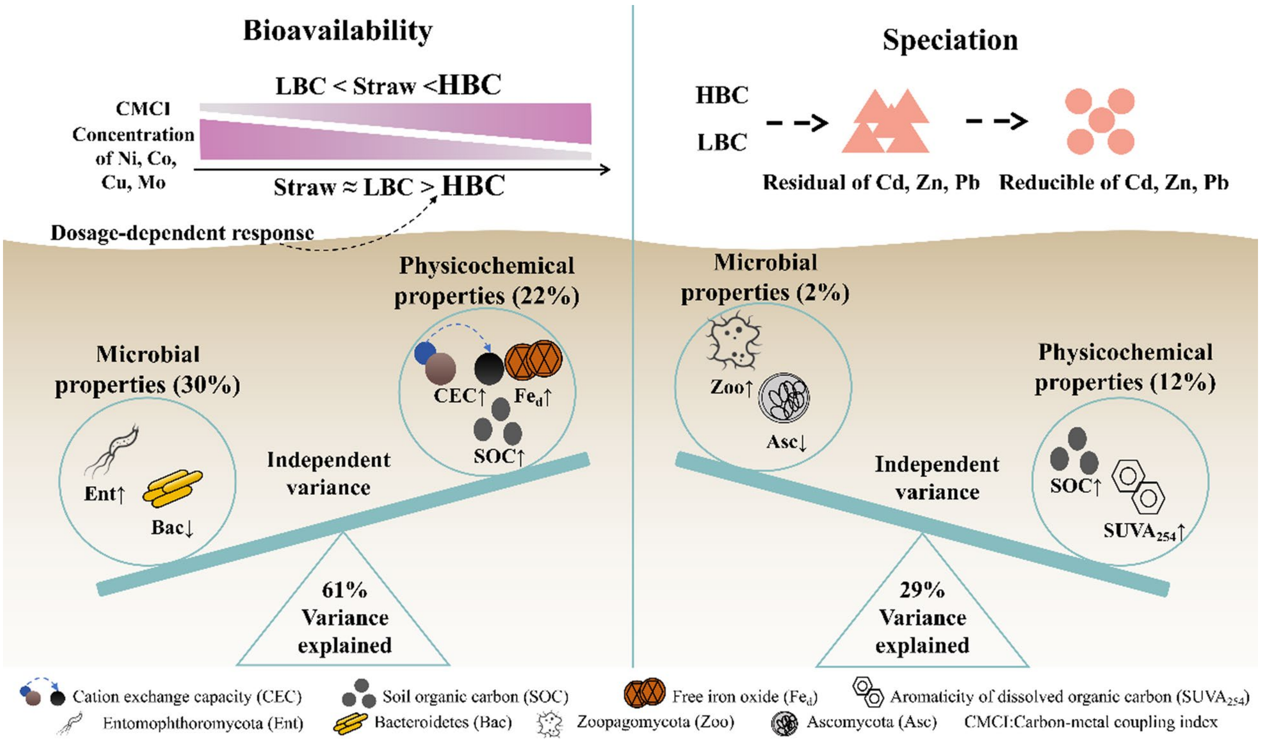

1 Introduction

Global agricultural ecosystems face severe challenges from heavy metal contamination. In China alone, the concentrations of heavy metals such as Cd, Pb, and Ni in nearly 20 million hectares of farmland (approximately one-fifth of the country's total farmland) exceed risk control values (Song et al. 2022). Due to their inherent toxicity, bioaccumulation properties, and resistance to degradation (Haghighizadeh et al. 2024; Liu et al. 2024; Weng et al. 2024), heavy metal pollution continues to spread and triggers multiple ecological and health risks (Adnan et al. 2024). For example, 2.2–10% of surveyed rice samples nationwide have Cd content exceeding the specified maximum allowable level, which directly threatens human health through diet (Angon et al. 2024; Gao et al. 2024; Qin et al. 2021a, b). While carbon sequestration-focused agricultural practices are widely applied, they fall short in controlling heavy metal pollution, urgently requiring synergistic strategies to achieve the dual goals of carbon sequestration and pollution mitigation.

Biochar, defined as a carbon-based material with high specific surface area and porous structure (Fu et al. 2023), is increasingly recognized as a multifunctional amendment for environmental management. It can immobilize heavy metals (Shentu et al. 2022), remediate organic pollutants (Wang et al. 2025), and enhance carbon sequestration (Chen et al. 2024b) and soil fertility (Dong et al. 2025). Numerous studies have reported its short-term capacity to immobilize heavy metals in soil. For example, Zhang et al. (2021) demonstrated a progressive decrease in bioavailable Cu, Ni, and Pb concentrations with increasing biochar application rates, modulated by biochar-induced pH elevation and aging processes. Zhu et al. (2015) showed 29.6%, 26.3%, and 48.14% decreases in exchangeable Ni, Cu, and Cd fractions, respectively, at a 0.5% biochar application rate. The dominant short-term mechanisms include physical adsorption (Rehman et al. 2019), ion exchange (Qiu et al. 2021), and complexation (Dai et al. 2018). However, biochar pore structure collapse during field aging processes may lead to remobilization of previously adsorbed heavy metals (Chen et al. 2025a, b). Most existing studies remain confined to short-term laboratory conditions, highlighting the need for long-term field experiments to assess the persistence of metal immobilization by biochar. In addition, straw, as another widely used carbon management measure, can exert contrasting effects on heavy metals compared to biochar. By increasing the adsorption of dissolved organic carbon (DOC) and cellulose (Chen et al. 2020), straw may promote the mobility of heavy metals. However, the mechanisms underlying the contrasting long-term effects of biochar and straw on carbon sequestration and metal immobilization remain unclear. To date, the fundamental effect of biochar on heavy metals by altering soil properties has been widely recognized (El-Naggar et al. 2021; Meng et al. 2018). However, how these changes in physicochemical properties specifically affect the bioavailability and speciation of heavy metals over the long term requires further research. Moreover, microorganisms can also affect metals through mineral dissolution (Wang et al. 2017a, b), but most research focuses on microbial response to metal contamination (Zhang et al. 2016) and toxicity (Pan and Yu 2011) rather than their reverse regulatory roles. It is essential to study how biochar and straw affect heavy metal bioavailability and speciation over extended periods from the perspectives of soil physicochemical and microbial properties, and to clarify the synergistic interaction between physicochemical and microbial processes.

To address this knowledge gap, we conducted a 14-year field experiment in Shandong Province. By measuring the bioavailable concentrations and speciation of heavy metals through Diffusive Gradients in Thin-films (DGT) and the Community Bureau Reference (BCR) sequential extraction, and characterizing soil physicochemical and microbial properties, we aimed to answer three key scientific questions: (1) How do low and high dosages of biochar and straw differentially affect heavy metal bioavailability and speciation over the long term? (2) What are the pathways and relative contributions of soil physicochemical and microbial properties in driving changes in heavy metal bioavailability and speciation? (3) How can a carbon–metal coupling index be constructed to evaluate the long-term synergistic effects of biochar and straw amendments on heavy metal immobilization and carbon sequestration? Our study can provide insights for adjusting soil carbon management to achieve simultaneous carbon sequestration and pollution reduction.

2 Materials and methods

2.1 Study area

The field experiment was conducted at the North China Agro-Ecological Research Station in Huantai County, which is located in an agricultural intensive area of Shandong Province, between 36°51′50"N and 37°06′00"N latitude, and between 117°50′00"E and 118°10′40"E longitude, with a total area of 509 km^2. This region experiences a warm temperate continental monsoon climate with a mean annual temperature of 12.4 °C and precipitation of 600 mm, predominantly concentrated from June to August. The county's alluvial plain geomorphology, formed by the historic Yellow River sedimentation, features Fluvic Cambisol soils with surface soil comprising 70.8% sand, 26.9% silt, and 2.3% clay. The dominant cropping system follows a winter wheat-summer maize double-cropping rotation. Detailed environmental characteristics of the experimental site are documented in Chen et al. (2023b).

2.2 Field experiment design and sample collection

A 14-year field experiment was initiated in June 2007 with four treatments: control (no amendment), low biochar (LBC, 4.5 Mg ha^{-1} yr^{-1}), high biochar (HBC, 9.0 Mg ha^{-1} yr^{-1}), and straw (Straw, 15.0 Mg ha^{-1} yr^{-1}), each replicated three times. The LBC rate was determined based on biochar yield (~30%) from straw biomass. Biochar was produced by pyrolyzing crushed corn straw or rice husks at 360 °C for 24 h (Jinfu Biochar Co., Liaoning Province) and sieved to < 1 mm before application. Corn straw-derived biochar ($pH_{(CaCl2)} = 8.2$, C content = 657.3 g kg^{-1}) was applied from 2007 to 2012. Due to discontinued production, rice husk biochar ($pH_{(CaCl2)} = 6.31$, C content = 308.0 g kg^{-1}) was substituted post-2012. Soil sampling in March 2021 involved collecting three topsoil cores (0–20 cm depth) per plot, which were homogenized into composite samples. Fresh soils were sieved (< 2 mm) to remove roots and gravel and split into two subsamples: one stored at −80 °C for microbial analysis, and another air-dried for physicochemical characterization and metal bioavailability and speciation assays. All measurements included triplicate technical and analytical replicates. Divergent soil physicochemical and microbial properties across treatments (Gul et al. 2015; Siedt et al. 2021) likely generated distinct heavy metal bioavailability and speciation patterns under long-term carbon amendments.

2.3 Deployment and analysis of DGT

The bioavailable concentration of heavy metals in soil was determined using Diffusive Gradients in Thin-films (DGT). Unlike traditional methods that measure only the static equilibrium concentration between soil solid and liquid phases (such as $CaCl_2$ extraction), DGT is an in-situ technique that simulates the dynamic process of plant root absorption by artificially constructing a layer of diffusion gel (Gao et al. 2020; Wu et al. 2023). Heavy metal ions in soil solution diffuse freely through the diffusion gel and are adsorbed by the resin gel, resulting in a decrease in concentration. This reduction is supplemented by easily desorbed metals from the soil solid phase. The DGT device enables quantification of metal bioavailability by capturing this dynamic consumption-supplement process (Ding et al. 2016; Tian et al. 2018).

The DGT device employing cylindrical Chelex-100 binding gels (DGT Research Ltd., UK) was utilized to quantify the bioavailable concentration of heavy metals (Chen et al. 2023a, b), which has an exposure window of 2.54 cm^2, with resin gel and diffusion gel thicknesses of 0.50 mm and 0.78 mm, respectively. Soil pastes were prepared by moistening 60 g of air-dried, sieved (< 2 mm) soil to 70% water-holding capacity (WHC), incubating for 48 h, then adjusting to 100% WHC for 24 h. Triplicate DGT devices were vertically inserted into soil pastes to ensure intimate soil-filter membrane contact, followed by 24 h deployment at 25 ± 1 °C (Gao et al. 2020). Pistons were rinsed with ultrapure water to remove soil particulates before disassembly and resin gels were eluted with 1.5 mL of 1 M HNO_3 for 24 h. Soil solutions were obtained by centrifuging (3000 rpm, 15 min) and filtering through 0.45 μm membranes. Eluent heavy metal concentrations were determined by inductively coupled plasma mass spectrometry (ICP-MS; Agilent 7700x, USA). The bioavailable concentrations measured by DGT were calculated as follows (Xu et al. 2018):

$$M = \frac{C_e\left(V_{gel} + V_{acid}\right)}{f_e} \tag{1}$$

$$C_{DGT} = \frac{M \times \Delta g}{D \times A \times t} \tag{2}$$

where C_e (mg L^{-1}) is the bioavailable concentration of heavy metals in the eluent, V_{gel} (L) is the volume of the binding gel, V_{acid} (L) is the volume of the eluent, f_e is the elution factor for heavy metals, M is the mass accumulated on the binding gel, Δg is the combined thickness of the diffusive gel layer and filter membrane, D (cm^2 s^{-1}) is the diffusion coefficient of heavy metals at 25 °C, A (cm^2) is the surface area of the gel layer, and t (s) is the deployment duration. Bioavailable concentrations of Cd, Pb, Ni, Co, Cu, and Mo are presented in Table S1.

2.4 BCR sequential extraction

Total heavy metal content was determined by HNO_3–HF–H_2O_2 digestion (Sungur et al. 2014). Briefly, 0.04 g samples were digested in 10-mL polytetrafluoroethylene (PTFE) vessels with 2 mL concentrated HNO_3 and 0.2 mL H_2O_2. The vessels were then placed on a hotplate for 24 h to remove organic matter. Subsequently, the residues were treated with 1 mL of concentrated HNO_3 and 2 mL of concentrated HF, sonicated for 20 min, and sealed at 190 °C for 48 h. Evaporated residues were reconstituted in 1% HNO_3 (v/v) and analyzed by ICP-MS (Agilent 7700x, Agilent Technologies, USA) (Xu et al. 2018). The analysis of the speciation of heavy metals in soil was carried out using a modified three-step sequential extraction method (Rauret et al. 2001; Gao et al. 2017; Pueyo et al. 2008). We accurately weighed 0.5 g of the dry soil sample into a polypropylene centrifuge tube. Exchangeable fraction: 0.11 M acetic acid extraction (pH = 2.85). Reducible fraction: 0.5 M hydroxylamine hydrochloride (pH = 1.5). Oxidizable fraction: H_2O_2/1.0 M ammonium acetate (pH = 2–3) digestion. Residual phases were quantified by acid digestion of post-extraction solids (Gao et al. 2017). The exchangeable fraction, representing the most bioavailable speciation, includes ion-exchangeable and carbonate-bound metals susceptible to rhizosphere uptake (Ma et al. 2016). Reducible metals are immobilized through adsorption onto Fe/Mn oxides or incorporation into their crystalline matrices (Liu et al. 2023a, b). Oxidizable metals form stable complexes with organic ligands or sulfides, exhibiting limited bioavailability (Bogusz and Oleszczuk 2020). Residual metals are structurally encapsulated within silicate lattices, rendering them inert. Method accuracy was assessed using BCR-701 certified reference material, yielding recovery rates of 80–120%. Speciation data for Cd, Zn, Pb, Cu, Cr, and Ni are presented in Table S2.

2.5 Soil physicochemical and microbial characterization

Soil pH was determined using a pH meter (FE28-Standard, Mettler Toledo, Switzerland) in a 1:2.5 (w/v) soil-to-water suspension. Total carbon (TC) content was analyzed with an elemental analyzer (Vario EL Cube, Elementar, Germany). Soil organic carbon (SOC) was quantified after pretreating samples with 1 M HCl to remove carbonates, followed by elemental analysis. Soil inorganic carbon (SIC) was calculated as the difference between TC and SOC. Dissolved organic carbon (DOC) was extracted by shaking soil–water suspensions (1:5 w/v) for 24 h, then analyzed using a TOC analyzer (Sievers 900, SUEZ, USA). Notably, these operational procedures capture only the readily extractable DOC fraction, which may not fully represent in-situ DOC composition. UV–vis spectroscopy (200–800 nm, 1 nm resolution) of DOC was performed using a spectrophotometer (DR6000, Hach, USA). Cation exchange capacity (CEC) was measured using the barium chloride buffer solution method (Jaremko and Kalembasa 2014). Soil aggregates were fractionated using a modified dry-sieving protocol (Jiang et al. 2018), with microaggregates (MA) defined as particles < 0.25 mm. Density fractionation of MA (< 53 μm) isolated mineral-associated organic matter (MAOM; $\rho > 1.6$ g cm^{-3}) following Weng et al. (2018). Free iron oxides (Fe_d) were quantified using the citrate-bicarbonate-dithionite (CBD) extraction method (Lalonde et al. 2012), representing total pedogenic Fe oxides (amorphous + crystalline phases). Iron concentrations in extracts were determined by ICP-OES (iCAP

6300, Thermo Scientific, USA). Treatment-specific soil properties are summarized in Table S3.

To elucidate microbial regulation of heavy metal bioavailability and speciation, we quantified three microbial properties: enzyme activities, microbial biomass, and community structure. β − 1,4-glucosidase (BG) and β-N-acetylglucosaminidase (NAG) activities were determined using p-nitrophenyl-β-D-glucopyranoside and p-nitrophenyl-N-acetyl-β-D-glucosaminide substrates, respectively, following Paz-Ferreiro et al. (2012). Phospholipid fatty acids (PLFAs) were extracted from freeze-dried soils to assess microbial biomass, following the method of Bossio and Scow (1998). Quantification was performed using a gas chromatograph equipped with flame ionization detection (GC-FID; Agilent 7890B, USA). Peaks were identified using bacterial acid methyl ester standards and MIDI Sherlock® software (MIDI Inc., USA), with concentrations expressed as nmol g^{-1} dry soil. Microbial diversity and community composition were analyzed through 16S (bacteria) and ITS (fungi) gene amplicon sequencing (Wang et al. 2017a, b). Rarefaction curves approached saturation across treatments (Fig. S1), confirming sufficient sequencing depth for diversity characterization. Microbial properties under biochar/straw amendments are detailed in Table S4 and Fig. S2.

2.6 Partial least squares-structural equation modeling (PLS-SEM) and variance partitioning analysis (VPA)

We used the *plspm* package to construct a partial least squares-structural equation modeling (PLS-SEM) to investigate the direct and indirect effects of biochar/straw amendments on metal bioavailability/speciation (Chen et al. 2022). PLS-SEM has low demands regarding measurement scales, sample sizes, and less restrictive assumptions for data normality (Monecke and Leisch 2012). Multivariate techniques such as PCA combine data into a robust index by assigning weights to indicators (Mukherjee and Lal 2014). In contrast, the PLS regression method can calculate a set of optimal weights for these indicators based on the correlation between the indicators and the response variables, thereby integrating them into a composite index capable of predicting the response variable (Obade and Lal 2016). In addition, PLS-SEM can estimate unmeasured latent variables through multiple observed variables, and quantitatively analyze causal path relationships between latent variables or between observed variables and latent variables, which cannot be achieved by PCA and RDA (Li et al. 2024; Liengaard 2024). This model incorporated five latent variables—soil physicochemical properties, fungal properties, bacterial properties, bioavailability, and speciation—each represented by multiple observed variables. To mitigate multicollinearity, covariates with correlation coefficients < 0.8 and variance inflation factors (VIF) < 5 were retained following Smart PLS 4.0 calculations (Li et al. 2024). Model adequacy was evaluated using the goodness-of-fit (GOF) index, where values > 0.7 indicate excellent fit (Wang et al. 2016). In the results of PLS-SEM, the influence of latent variables is represented by the combination of path coefficients and significance levels (*p* values) (Cheah et al. 2021). Variance partitioning analysis (VPA) using the *vegan* package quantified the relative contributions of soil properties versus microbial properties to metal bioavailability/speciation variances (Qin et al. 2021a, b).

2.7 Construct Carbon–Metal Coupling Index (CMCI)

The study constructed the CMCI using the entropy weight method (Lu et al. 2019) to evaluate the comprehensive effectiveness of different carbon management strategies in terms of carbon sequestration capacity and heavy metal immobilization potential. This index integrated two core dimensions, namely the carbon sequestration capacity (characterized by the Carbon Sequestration Efficiency (CSE)) and the heavy metal immobilization potential (characterized jointly by the reduction rate of bioavailable concentration (ΔBC) and the increase in the proportion of stable speciation (ΔSS)). After data were normalized using min–max scaling to eliminate dimensional discrepancies, the entropy values (e_j) and coefficient of variation (d_j) of each indicator were calculated. After obtaining the weights, the composite CMCI score was computed using a linear weighted model (He et al. 2017):

$$CMCI_i = \sum w_j \times x_{ij}^{norm} \tag{3}$$

where w_j is the weight of CSE, ΔBC and ΔSS and x_{ij}^{norm} is the normalized values of CSE, ΔBC and ΔSS in the HBC, LBC and Straw treatments. The specific calculations of CSE, ΔBC, ΔSS, normalization and weights are shown in the Supplementary Information.

2.8 Statistical analyses

Spearman correlation analyses were performed in R v4.3.1 (https://www.r-project.org/) using the *heatmap* and *corrplot* packages to assess relationships between heavy metal bioavailability/speciation and soil properties (pH, SOC, SIC, DOC, $SUVA_{254}$, CEC, MA, MAOM, Fe_d) and microbial properties (BG, NAG, PLFAs, α-diversity indices, phylum-level abundances) (Zhou et al. 2024).

3 Results and discussions

3.1 Effects of biochar and straw on heavy metal bioavailable concentration

3.1.1 Heavy metal bioavailable concentration

The bioavailable concentrations of six heavy metals (Cd, Pb, Ni, Co, Cu, Mo) were quantified in the four tested soils. The bioavailable concentrations of Cd and Pb remained below 0.1 mg L^{-1} across treatments. Ni, Co, and Cu exhibited moderate bioavailability, ranging from 0.40 to 0.52 mg L^{-1}, while Mo demonstrated the highest bioavailability (1.93 mg L^{-1}). The bioavailable concentrations of heavy metals fell within the lower range of values reported in the literature (Chen et al. 2021).

For polluting elements such as Cd, Pb, Ni, HBC amendment induced slight reductions in bioavailability by 2–5%. Conversely, LBC increased their bioavailability by 14%, 11%, and 8%, respectively. Straw incorporation elevated Cd and Ni bioavailability by 6% and 33% while reducing Pb bioavailability by 18% (Fig. 1). For biogenic elements including Co, Cu, Mo (Ma et al. 2017), LBC treatment reduced the bioavailability of Co and Cu by 36% and 28%, respectively, while Mo bioavailability remained unchanged. HBC induced further significant reductions in bioavailability by 91%, 31%, and 55% for Co, Cu, and Mo, respectively. In contrast, straw amendment decreased Cu bioavailability by 23% but increased Co and Mo bioavailability by 17% and 58% (Fig. 1).

Collectively, these results demonstrated that HBC effectively immobilized heavy metals, substantially reducing their bioavailability. LBC exhibited limited immobilization capacity and even increased the bioavailability of polluting elements. Traditional straw incorporation generally enhanced metal bioavailability, except for Pb and Cu. These results indicated that biochar had more effective immobilization than straw, with enhanced performance at higher application rates. This finding was supported by Li et al. (2025), who reported that the dosage of biochar had a negative correlation with the bioavailability of Cd, Pb, Ni, and Cu ($p < 0.01$). Our results highlighted the superior

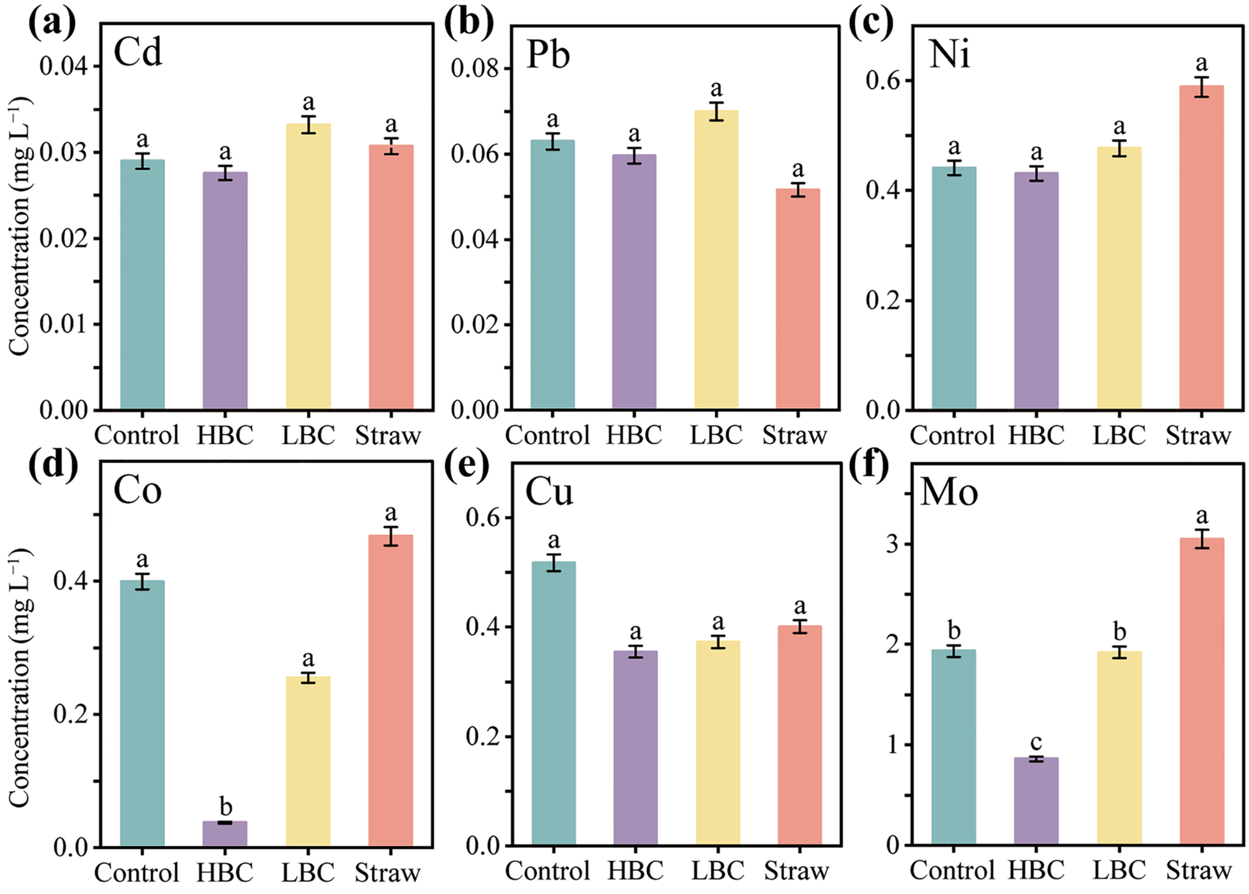

Fig. 1 Bioavailable heavy metal concentrations of Cd (**a**), Pb (**b**), Ni (**c**), Co (**d**), Cu (**e**) and Mo (**f**) in soils amended with biochar and straw. Control, no biochar or straw addition, HBC: high biochar addition group, 9.0 Mg ha^{-1} yr^{-1}; LBC: low biochar addition group, 4.5 Mg ha^{-1} yr^{-1}; straw: straw addition group, 15.0 Mg ha^{-1} yr^{-1}. Different lowercase letters denote significant differences from one-way ANOVA

ability of biochar, especially at a high application rate, to remediate heavy metal contaminated agricultural soil in comparison with straw amendment.

3.1.2 Impact of soil physicochemical properties on heavy metal bioavailable concentration

The correlation analysis revealed that the bioavailable concentrations of Ni and Mo were negatively correlated with CEC ($p < 0.05$, $p < 0.01$, respectively, Fig. 2a). This indicated that the immobilization mechanism of

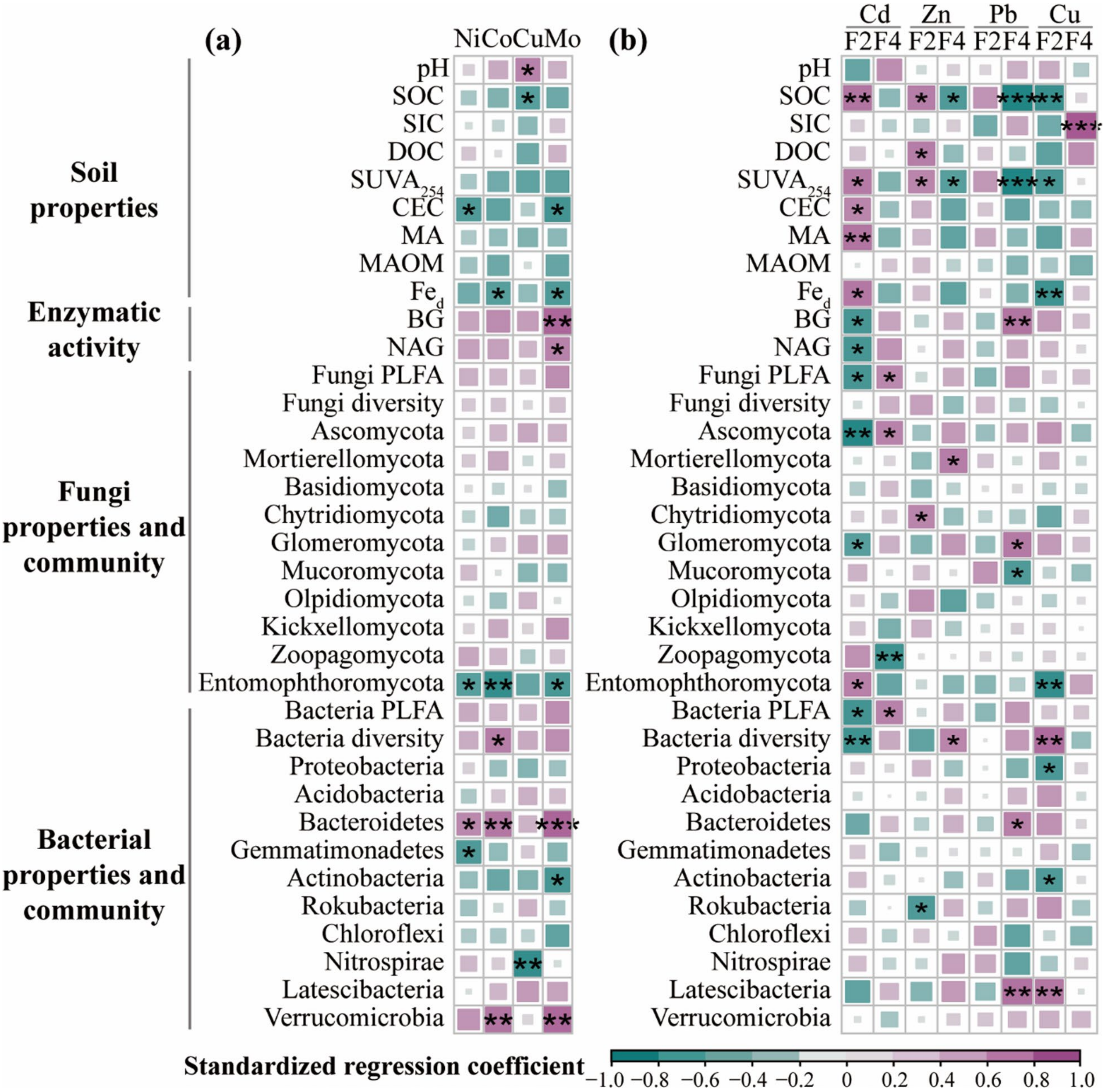

Fig. 2 Spearman correlations between **a** bioavailable heavy metal concentrations and **b** speciation fractions with biotic/abiotic factors under biochar/straw amendments. SOC, soil organic carbon; SIC, soil inorganic carbon; DOC, soil dissolved organic carbon; $SUVA_{254}$, Specific Ultraviolet Absorbance at 254 nm; CEC, soil cation exchange capacity; MA, Microaggregate; MAOM, Mineral-Associated Organic Matter; Fe_d, free iron oxide; BG, β-1,4-glucosidase; NAG, β-N-acetylglucosaminidase; PLFA, phospholipid fatty acid. The Shannon index was used to evaluate the α-diversity of bacterial and fungal communities; F2, reducible fraction, mg kg^{-1}; F4, residual fraction, mg kg^{-1}; Statistical significance: * $p < 0.05$, ** $p < 0.01$, *** $p < 0.001$

Ni and Mo by biochar could arise from elevated CEC. The increased CEC under biochar application directly enhanced ion exchange adsorption between soil colloids and Ni^{2+} by providing more adsorption sites, effectively sequestering Ni^{2+} on colloidal surfaces (Nkoh et al. 2022). Meanwhile, biochar-amended soil indirectly attracted additional MoO_4^{2-} anions for surface complexation to maintain charge balance (Wei et al. 2023a, b), thereby facilitating the further stabilization of Mo. Furthermore, the elevated CEC could further contribute to Ni and Mo immobilization by reducing desorption through electrostatic reinforcement (Gjoka et al. 2011).

Besides, the bioavailable concentrations of Co and Mo were negatively correlated with Fe_d ($p < 0.05$, Fig. 2a). This is understandable, as Fe_d could contribute to heavy metal immobilization through two pathways, such as providing abundant adsorption sites (Cheng et al. 2023) and forming stable hydroxyl-metal complexes by surface hydroxyl functional groups (Liang et al. 2022). Biochar amendment significantly enhanced Fe_d content (Table S3), which could facilitate Co^{2+} immobilization by $Co(OH)_2$ precipitation. Conversely, straw treatment decreased CEC while maintaining relatively stable Fe_d levels (Table S3), leading to an increase in the bioavailability of Ni, Co, and Mo.

In addition, the bioavailability of Cu was positively correlated with pH ($p < 0.05$) and negatively correlated with SOC ($p < 0.05$, Fig. 2a). This indicated that biochar-induced decrease in soil pH may promote the encapsulation of Cu^{2+} ions by accelerating the reaction between Cu^{2+} and chloride (Cl^-) ions to form complexes (e.g., $[CuCl_4]^{2-}$) (Tian et al. 2022). On the other hand, the biochar-induced increase in SOC content could strengthen the binding of Cu^{2+} with carboxyl and phenolic hydroxyl groups in SOC to form poorly soluble complex precipitates (Table S3; Shen et al. 2022), leading to a decrease in the bioavailability of Cu.

Overall, the immobilization of Ni, Co, and Mo was driven by CEC-mediated ion exchange adsorption and Fe_d-dominated hydroxyl complexation, while the bioavailability of Cu was regulated by pH-SOC-synergized coordination precipitation. Biochar enhanced the immobilization efficiency of Ni, Co, Cu, and Mo by amplifying the CEC-Fe_d-SOC system, whereas straw amendments exacerbated heavy metal mobilization risks through organic ligand release.

3.1.3 Impact of soil microbial properties on heavy metal bioavailable concentration

β-1,4-glucosidase (BG) and β-N-acetylglucosaminidase (NAG) enzymatic activities exhibited positive correlations with Mo bioavailability ($p < 0.05$ and $p < 0.01$, respectively, Fig. 2a). This phenomenon was attributed to enzyme-mediated acceleration of organic matter decomposition, generating low-molecular-weight organic compounds (e.g., soluble carboxylates and amino acids) that form bioavailable Mo-organic complexes (Li et al. 2022). Biochar amendment reduced Mo bioavailability by lowering soil pH, which suppressed enzymatic activity (Table S4). In contrast, straw incorporation elevated enzyme activity through enhanced organic matter inputs (Li et al. 2021), consequently increasing Mo bioavailability (Table S4).

The correlation analysis further indicated that Entomophthoromycota was negatively correlated with the bioavailability of Ni, Co, and Mo, while Bacteroidetes was positively correlated with them ($p < 0.05$, Fig. 2a). Similarly, Verrucomicrobia was positively correlated with the bioavailability of Co and Mo ($p < 0.01$, Fig. 2a). These results suggest that biochar-induced enrichment of Entomophthoromycota and the decline in Bacteroidetes and Verrucomicrobia abundances could explain the reduced bioavailability of Ni, Co, and Mo (Fig. S2). Specifically, Entomophthoromycota could adsorb Ni^{2+}, Co^{2+}, and MoO_4^{2-} through its hyphae with larger specific surface area (Bano et al. 2018; Wang et al. 2021a, b), and its pathogenicity may further suppress microbial groups involved in Ni/Co/Mo mobilization (Gryganskyi et al. 2012). The decrease in Bacteroidetes abundance could reduce organic ligand availability (Cui et al. 2021) and small molecular organic acids production (Chen et al. 2024b, a), thereby limiting soluble Ni/Co/Mo-organic complexes. Furthermore, Bacteroidetes could consume oxygen and create localized anaerobic microsites, and their reduced abundance weakens anaerobic respiration using heavy metals as electron acceptors (Upadhyay et al. 2025). This process typically dissolves metal oxides and releases soluble metals, such as iron-manganese oxides. Verrucomicrobia could promote Co^{2+}/MoO_4^{2-} release from minerals by secreting organic acids (Naznin et al. 2017), as well as form bioavailable metal complexes by producing extracellular polymeric substances (Fan et al. 2024). Other bacterial phylum, including Gemmatimonadetes and Actinobacteria, could also negatively impact Ni and Mo bioavailability ($p < 0.05$, Fig. 2a), potentially through adsorption, complexation-precipitation, and microbial community restructuring (Liu et al. 2023a, b; Wei et al. 2023a, b).

The availability of Cu was negatively related to Nitrospirae abundance ($p < 0.01$, Fig. 2a). Biochar and straw amendments provided abundant substrates for Nitrospirae, enhancing its proliferation and consequently reducing Cu bioavailability (Fig. S2). This is because Nitrospirae can limit Cu^{2+} participation in redox reactions by competitively sequestered electrons (Sun et al. 2021). On the other hand, Nitrospirae activities provide an effective nitrogen source for soil microorganisms, which may promote the formation of SOC (Zhang et al. 2025). SOC immobilized Cu^{2+} through complexation to form a stable Cu-organic complex, thereby reducing the bioavailability of Cu.

Collectively, Entomophthoromycota, Bacteroidetes, Verrucomicrobia, and Nitrospirae reduced metal bioavailability via hyphal adsorption, organic ligand complexation, metabolite mediation, and electron transfer interference. Biochar immobilized Ni, Co, Cu, and Mo through enriching Entomophthoromycota and Nitrospirae while suppressing Bacteroidetes and Verrucomicrobia. Conversely, straw amendments promoted the mobilization of Ni, Co, and Mo through facilitating enzyme-activated redox cycling and stimulating organic ligand complexation driven by the proliferation of Bacteroidetes and Verrucomicrobia.

3.2 Effects of Biochar and Straw on Heavy Metal Speciation

3.2.1 Heavy metal speciation

BCR sequential extraction revealed distinct changes in the speciation of Cd, Zn, Pb, Cu, Cr, and Ni under biochar and straw amendments (Fig. 3). Cd, Zn, Pb, and Cu predominantly occurred in reducible (10–44%) and residual fractions (29–84%). Biochar amendment increased reducible fractions by 1–18% while decreasing residual fractions by 2–18% (except for Cu). In contrast, straw elevated reducible Cd and Zn by 1% and 3%, while slightly decreasing (by 2%) or maintaining the residual fractions. However, straw reduced reducible Pb and Cu fractions by 1% and 2%, respectively, accompanied by 2–3% increases in their residual fractions.

Cr and Ni were primarily distributed in oxidizable (19–30%) and residual fractions (66–73%). HBC increased oxidizable Cr and Ni by 3% and 1%, respectively, while reducing residual fractions by 2%. LBC had no effect on Cr speciation, whereas straw decreased Cr oxidizable fractions by 2% and increased residual fractions by 4%. Both LBC and straw reduced Ni oxidizable fractions by 2% and increased residual fractions by 2%.

These results demonstrated that biochar amendments increased the reducible or oxidizable phases of Cd, Zn, Pb, Cr, and Ni, thereby maintaining their bioavailability at relatively low levels and achieving effective immobilization of these metals (Fig. 4). In contrast, straw exhibited no significant impact on heavy metal speciation, because percentage changes in concentrations across all metal speciation remained below 5%. Beyond concentration changes, our findings confirmed that biochar can alter the speciation of heavy metals, highlighting the importance of monitoring speciation changes during heavy metal immobilization processes to mitigate associated risks.

3.2.2 Impact of soil physicochemical properties on heavy metal speciation

The reducible Cd and Zn fractions exhibited positive correlations with SOC and $SUVA_{254}$ (indicator of DOC aromaticity) ($p < 0.05$), and the reducible Cd fraction showed positive correlation with microaggregate ($p < 0.01$, Fig. 2b). This can be attributed to the ability of Cd^{2+} and Zn^{2+} to interact with organic ligands and aromatic compounds in SOC, forming soluble Cd^{2+} and Zn^{2+}-organic complexes (Egli et al. 2010). These complexes exhibited high bioavailability, thereby increasing the reducible fraction of Cd and Zn. In addition, microaggregates provided abundant adsorption sites, and Cd^{2+} enhances the reducible fraction by forming soluble complexes with carboxyl and phenolic hydroxyl groups (Wang et al. 2021a, b).

The residual Pb and reducible Cu fractions showed negative correlations with SOC and $SUVA_{254}$ ($p < 0.05$, Fig. 2b). This is because Cu^{2+}, with strong coordination ability, can be stabilized as precipitates of relatively low bioavailability, which could lead to a decrease in the Cu reducible fraction (Fan et al. 2015). Meanwhile, SOC can stimulate the release of Pb^{2+} from the residual fraction, since the functional groups of SOC can form strong chemical bonds with Pb^{2+} (Tuo et al. 2024). Furthermore, reducible Cu negatively correlated with Fe_d ($p < 0.01$), while residual Cu positively correlated with SIC ($p < 0.001$, Fig. 2b). This is due to the fact that the reductive dissolution of Fe_d to Fe^{2+} can reduce Cu (II) to less mobile Cu(I) (Liu et al. 2020), whereas carbonate minerals can form insoluble $Cu_2(OH)_2CO_3$ with Cu^{2+} (Rizwan et al. 2021).

We showed that biochar amendment promoted the transformation of Cd, Zn, and Pb from the residual fraction to the reducible fraction, whereas it facilitated the transformation of Cu from the reducible to the residual fraction, maintaining their relatively low bioavailability (Fig. 3). Three mechanisms associated with physicochemical properties may help explain this transformation: (1) SOC and $SUVA_{254}$ drove Cd/Zn reducible fraction enrichment by organic ligand complexation, while microaggregate adsorption promoted Cd mobilization. (2) Pb^{2+} was released from residual fractions by its strong chemical bonding with functional groups. (3) Fe_d-mediated redox transformations and SIC precipitation stabilized residual Cu.

3.2.3 Impact soil microbial properties on heavy metal speciation

Based on microbial analysis, we found that reducible Cd negatively correlated with fungal PLFA biomass, bacterial PLFA biomass and Ascomycota relative abundance ($p < 0.05$), while residual Cd was positively correlated with them (all $p < 0.05$, Fig. 2b). In addition, the residual

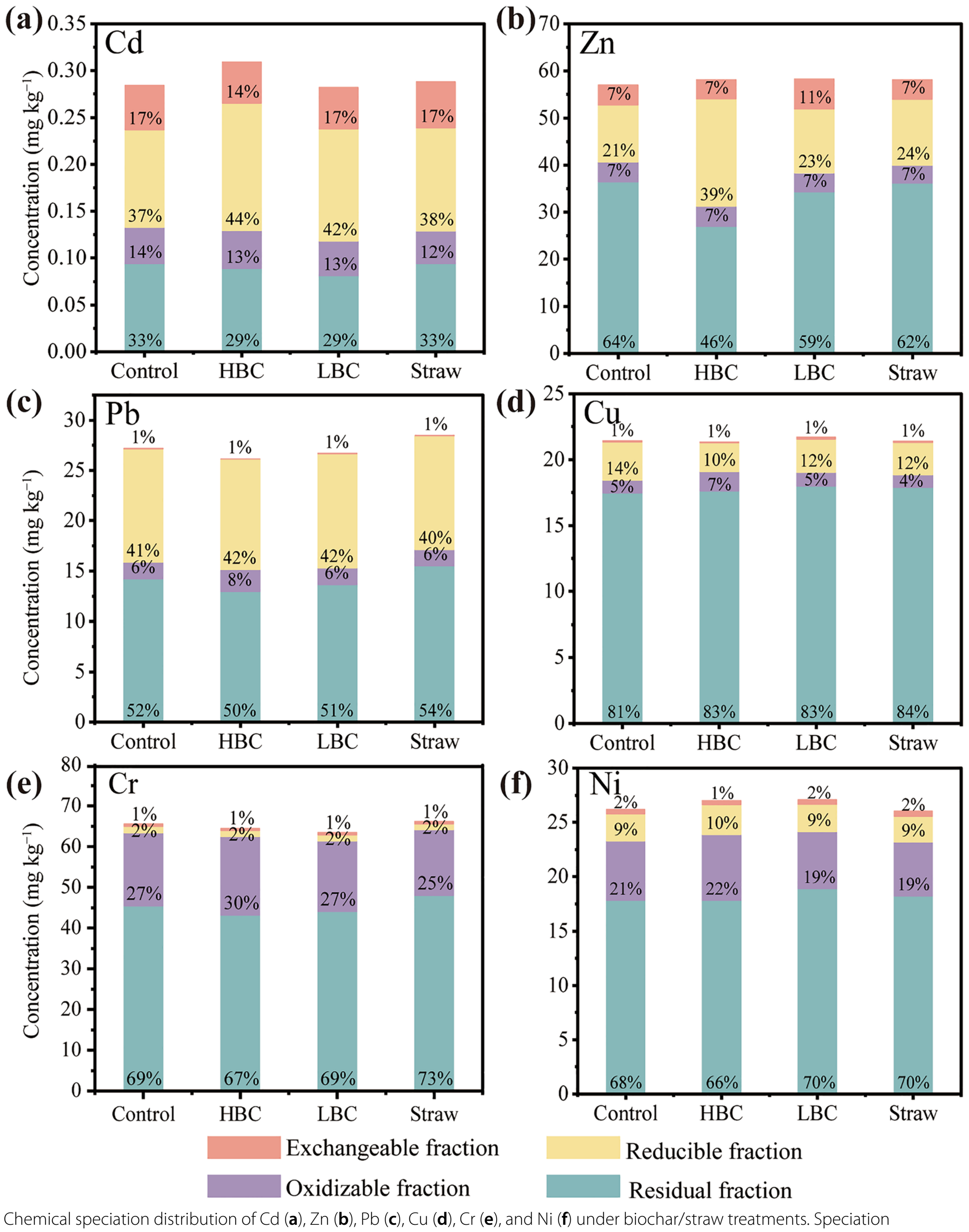

Fig. 3 Chemical speciation distribution of Cd (**a**), Zn (**b**), Pb (**c**), Cu (**d**), Cr (**e**), and Ni (**f**) under biochar/straw treatments. Speciation including exchangeable, reducible, oxidizable and residual fractions. Values denote percentage contributions to total metal content

Cd was negatively correlated with the relative abundance of Zoopagomycota ($p < 0.01$). This indicated that the speciation of Cd can be attributed to two microbial processes: (1) Ascomycota reduced the reducible and increased the residual fraction of Cd through secreting metabolites which stimulate the formation of Cd-organic acid precipitation (Tuan et al. 2018). Specifically, Cd^{2+} forms cadmium oxalate precipitation with reduced oxalic

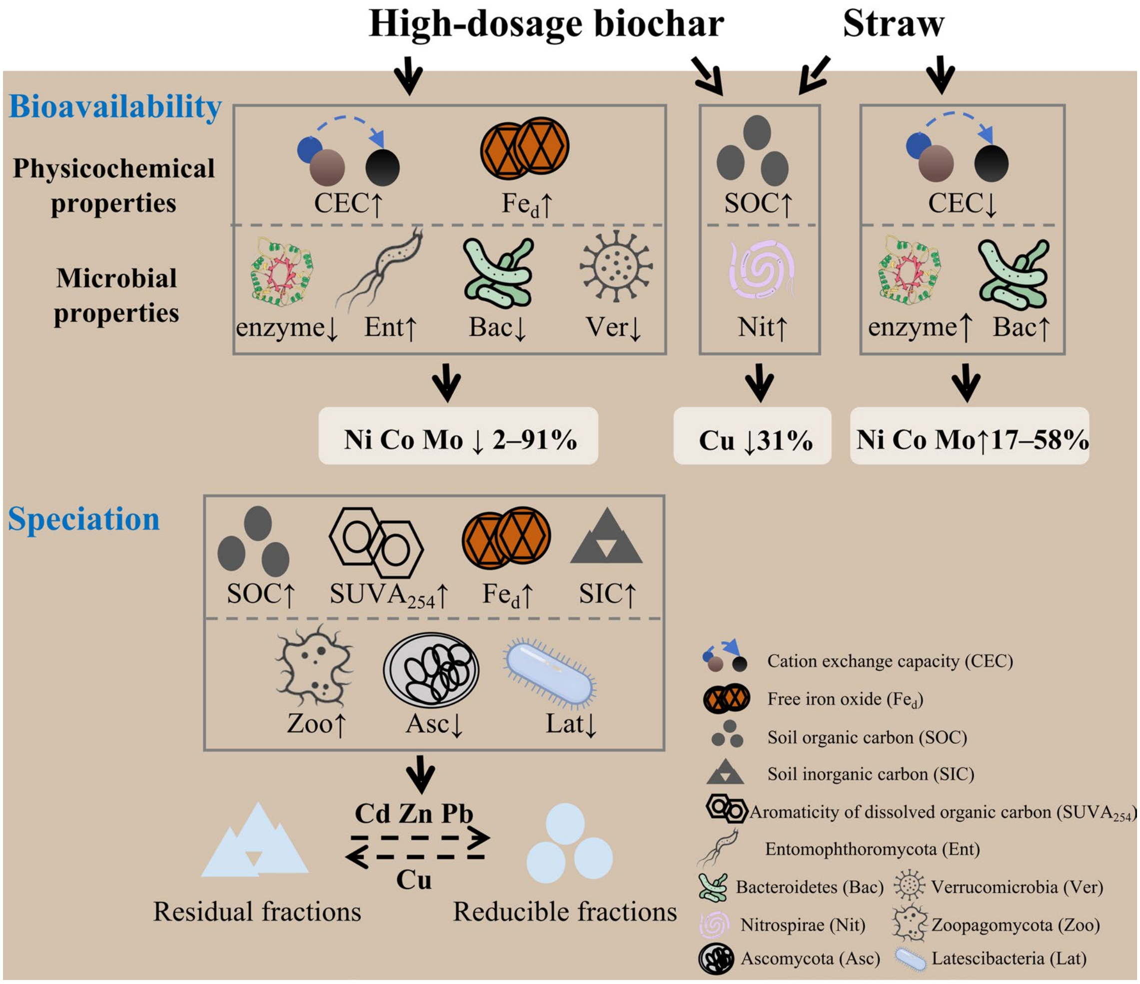

Fig. 4 Mechanisms of biochar and straw amendments on heavy metal bioavailability and speciation driven by soil physicochemical and microbial processes

acid secreted by Ascomycota (Xie et al. 2021). Meanwhile, Ascomycota promoted Cd^{2+} to exist in minerals in the form of residual fraction by utilizing other inorganic components in the environment (Lin et al. 2019). (2) Zoopagomycota reduced the residual Cd by dissolving Cd precipitates to release Cd^{2+} (Zhu et al. 2023). Additionally, it physically disrupted the mycelial encasements formed by Ascomycota (Hurdeal et al. 2021). Indeed, our results demonstrated that biochar decreased the abundance of Ascomycota but increased that of Zoopagomycota (Fig. S2), which led to immobilization of Cd by locking it in low-mobility Fe–Mn oxides.

The residual fraction of Pb and the reducible fraction of Cu were positively correlated with the relative abundance of Latescibacteria ($p < 0.01$). Latescibacteria dominates the mineralization of Pb^{2+} with inorganic components (Li et al. 2013), promoting the formation of $PbCO_3$ precipitates. Moreover, Latescibacteria-derived copper oxidase enzymes oxidized Cu(I) to Cu (II) (Irawati et al. 2021). The addition of biochar reduced the residual fraction of Pb and the reducible fraction of Cu (Fig. 3), possibly through inhibiting the Pb biomineralization and Cu biooxidation processes dominated by Latescibacteria.

Overall, biochar drove the transformation of Cd and Pb from residual to reducible fractions, while stabilizing Cu from reducible to residual fractions, maintaining their low bioavailability through two microbial pathways: (1) suppressing Ascomycota-mediated Cd precipitation and activating Zoopagomycota-driven Cd release; (2) inhibiting Latescibacteria-dominated Pb biomineralization and Cu biooxidation.

3.3 PLS-SEM and VPA analyses of Heavy Metal Bioavailability and Speciation Regulation

PLS-SEM analysis indicated that soil properties and microbial properties were important predictors of changes in the bioavailable concentration and speciation of heavy metals after the addition of biochar and straw. Both microbial properties and soil properties had direct positive effects on the bioavailable concentration and speciation of heavy metals, respectively (Fig. 5a). For the bioavailable concentration, soil physicochemical properties also showed an indirect effect by negatively affecting bacterial characteristics. Specifically, biochar and straw amendments directly influenced metal bioavailability through modulation of bacterial PLFA biomass and phylum-specific abundances (path coefficient (PC) = 0.768, $p < 0.01$), with Bacteroidetes identified as the primary driver of metal immobilization (PC = 0.883; Fig. 5a). Soil properties were not the main factor contributing to the

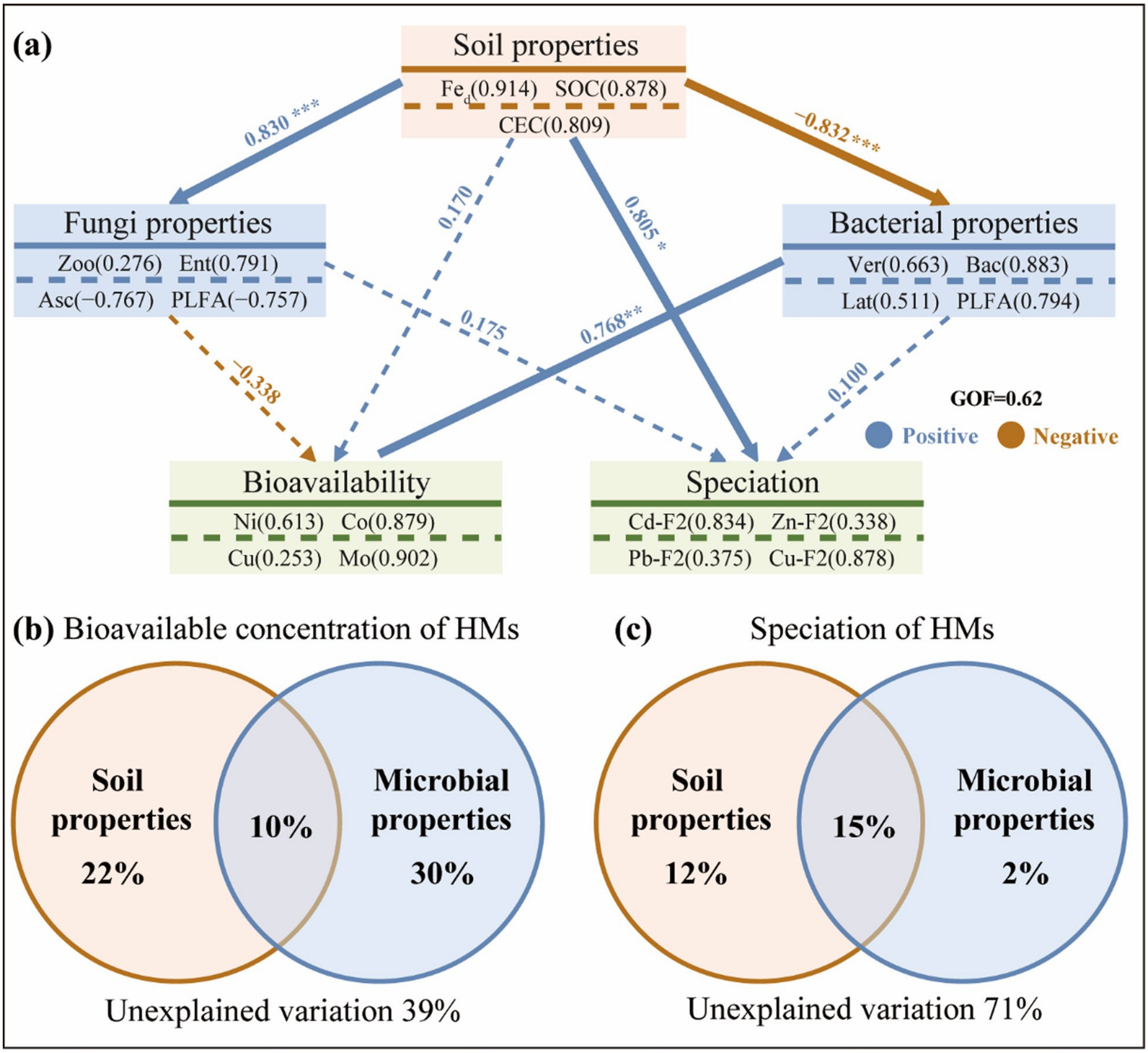

Fig. 5 Mechanistic drivers of heavy metal bioavailability and speciation under biochar and straw amendments. **a** Partial Least Squares Structural Equation Modeling (PLS-SEM) delineating direct (solid arrows) and indirect (dashed arrows) effects of biotic and abiotic factors. Variance partitioning analysis quantifying independent and shared contributions of soil properties (**b**) and microbial traits (**c**). Blue and orange arrows denote positive and negative causal relationships, respectively. Standardized path coefficients are annotated adjacent to arrows. Model fit: GOF = 0.62. Arrows denote causal directions (blue: positive; orange: negative). Soil properties: cation exchange capacity (CEC), free iron oxides (Fe$_d$), soil organic carbon (SOC); Fungal traits: phospholipid fatty acids (PLFA), Ascomycota (Asc), Entomophthoromycota (Ent); Bacterial traits: PLFA, Bacteroidetes (Bac), Verrucomicrobia (Ver), Latescibacteria (Lat). Bioavailability: Ni, Mo, Co, Cu (mg L^{-1}); Speciation: Cd-F2, Zn-F2, Pb-F2, Cu-F2 (F2: reducible fraction; mg kg^{-1}). Statistical significance: *$p < 0.05$, **$p < 0.01$, ***$p < 0.001$. Values in overlapping regions represent covarying effects, while values within circles denote independent contributions in (**b**) and (**c**)

decrease in the bioavailable concentration of heavy metals (PC = 0.170, $p > 0.05$, Fig. 5a). Regarding metal speciation, physicochemical properties (SOC, CEC, Fe_d) directly impacted the changes of the reducible fraction of heavy metals (PC = 0.805, $p < 0.05$, Fig. 5a), whereas microbial communities exerted indirect effects. SOC and Fe_d emerged as dominant regulators of speciation shifts (PC = 0.878 and 0.914, respectively; Fig. 5a). Consistent with the aforementioned results of correlation analysis, microbial properties dominated the bioavailable concentration of heavy metals, while the physicochemical properties of the soil were the key factors causing changes in the speciation of heavy metals (Fig. 2).

VPA analysis was further adopted to quantify the relative contributions of soil properties and microbial properties to heavy metal bioavailability (Fig. 5b) and speciation (Fig. 5c) shifts under biochar and straw amendments. Soil physicochemical properties and microbial properties explained 61% of the variance in metal bioavailability, and 29% in metal speciation. Microbial properties (30%) were more important factors than soil properties (20%) in explaining the bioavailable concentration of heavy metals (Fig. 5b). By contrast, soil properties (12%) had a higher degree of explanation for the speciation compared to microbial properties (Fig. 5c). Integrated with PLS-SEM results, these findings demonstrate that biochar-induced metal immobilization arises from physicochemical-microbial interactions: reduced bioavailability by suppression of Bacteroidetes and enhanced reducible fractions (through elevated SOC and Fe_d) coupled with reduced residual fractions, collectively stabilizing metals.

3.4 Potential of biochar for synergistic metal immobilization and carbon sequestration

Previous studies have predominantly assessed biochar and straw amendments through a singular perspective of either carbon sequestration or pollution remediation (Ji et al. 2022; Wang et al. 2023; Zhong et al. 2023). This research integrated carbon sequestration data to reveal the potential of biochar for synergistic carbon sequestration and heavy metal immobilization (Chen et al. 2023a, b, 2025a). Four well-recognized mechanisms explain the carbon sequestration achieved by biochar addition. First, biochar itself is rich in highly condensed aromatic structures, decreasing substrate degradability, imposing greater energetic barriers to microbial decomposition, thereby inhibiting carbon mineralization while increasing SOC content (Chen et al. 2025a, b; Wang et al. 2023). Second, biochar promoted mineral-associated organic matter formation and free iron oxide content, improving the physical protection of both native and biochar-derived C (Chen et al. 2025a, b; Qin et al. 2019). Third, microbial analysis showed that biochar suppressed microbial activity of SOC decomposition, such as the decrease in both fungal and bacterial PLFAs and extracellular enzyme activity, which reduced carbon decomposition (Chen et al. 2023a, b; Yang et al. 2025). In addition, the experiments showed that biochar could directly adsorb CO_2 by its micropore structure (Cao et al. 2023). In contrast, as a readily degradable organic carbon source, straw application stimulated microbial and enzyme activity, accelerated the mineralization of SOC from the added straw and the original soil (Fig. S3).

By constructing a carbon–metal coupling index using the entropy weight method, this study found that HBC achieved the highest composite score (0.703), significantly outperforming LBC (0.360) and Straw (0.396), demonstrating its optimal dual benefits in carbon sequestration and heavy metal immobilization (Table S5). Specifically, despite receiving the highest exogenous carbon input (27.63 g kg^{-1}), straw incorporation exhibited the lowest CSE (12%), whereas HBC and LBC (17.94 and 8.97 g kg^{-1}, respectively) achieved significantly higher CSE values of 63% and 55%, highlighting the superior carbon sequestration capacity of biochar compared to straw under equivalent field conditions.

Regarding heavy metal immobilization, HBC significantly reduced bioavailable concentrations ($\Delta BC = 32\%$), whereas LBC showed limited efficacy ($\Delta BC = 5\%$), and Straw increased bioavailability ($\Delta BC = -12\%$). These findings prove high-dosage biochar's long-term efficacy in simultaneously immobilizing metals and sequestering carbon. This highlights the need to adjust biochar application strategies to achieve multiple ecosystem functions and enhance agricultural sustainability.

4 Conclusion

This study demonstrated that HBC more effectively reduced the bioavailable concentration of heavy metals by 2–91% than LBC by 1–36%. Straw amendment increased bioavailability by 6–58%, except for Pb and Cu. Both HBC and LBC drove residual fractions of Cd, Zn, and Pb to reducible fractions with respective variation of 1–18% and 1–5%, whereas straw exhibited no significant impact (< 5% variation). PLS-SEM and VPA analyses showed that soil physicochemical and microbial properties jointly regulated heavy metal bioavailability with 61% of variance explained and speciation with 29% explained. Among them, the primary determinant of bioavailability was microbial properties, with an independent variance contribution of 30%, and that for speciation was physicochemical properties with 12%. When evaluating the carbon–metal coupling index, we found that HBC (0.703) outperformed LBC (0.361) and straw (0.396) in immobilizing heavy metals and sequestering carbon.

Our study revealed the dominant role of microbial processes in long-term regulation of heavy metal bioavailability, and proposed high-dose biochar as a preferred strategy to achieve agricultural carbon neutrality and heavy metal pollution control. However, this study has certain limitations: it is difficult to reveal the dynamic process of biochar aging and its heavy metal immobilization effect based on the end-state measurement after 14 years. Future research should further clarify the mechanism through long-term dynamic sampling, and provide more scientific basis for the long-term application of biochar in agricultural ecosystems to achieve heavy metal immobilization and carbon sequestration.

Supplementary Information

The online version contains supplementary material available at https://doi.org/10.1007/s42773-025-00553-0.

Supplementary material 1

Acknowledgements
The authors thank for the financial support by the National Science Foundation for Distinguished Young Scholars (42125703), National Natural Science Foundation of China (42530705, T2421005, 42507300), and China Postdoctoral Science Foundation (2025T180329, 2024M760247).

Author contributions

All authors contributed intellectual input and assistance to this study. Ke Sun and Yalan Chen initiated the project. Investigation and methodology were performed by Mengmeng Ma, Yunqian Zhang, Qiwen Ma, Zhibo Wang, Zhangliu Du, and Yalan Chen. Data analyses were performed by Mengmeng Ma, Yunqian Zhang and Yalan Chen. The first draft of the manuscript was written by Mengmeng Ma. Ke Sun, Yalan Chen, Qun Gao, Fei Wang and Bo Gao reviewed the results and provided feedback on the manuscript.

Funding
This work was supported by the National Science Foundation for Distinguished Young Scholars (42125703), National Natural Science Foundation of China (42530705, T2421005, 42507300) and China Postdoctoral Science Foundation (2025T180329, 2024M760247).

Data availability

The datasets used or analyzed during the current study are available from the corresponding author upon reasonable request.

Declarations

Competing interests

The authors declare no competing interest.

Author details

[1]State Key Laboratory of Regional Environment and Sustainability, School of Environment, Beijing Normal University, Beijing 100875, China. [2]Beijing Key Laboratory of Biodiversity and Organic Farming, College of Resources and Environmental Sciences, China Agricultural University, Beijing 100193, China. [3]State Key Laboratory of Simulation and Regulation of Water Cycle in River Basin, China Institute of Water Resources and Hydropower Research, Beijing 100038, China.

Received: 27 July 2025 Revised: 18 November 2025 Accepted: 21 November 2025

References

Adnan M, Xiao B, Ali MU, Xiao P, Zhao P, Wang H, Bibi S (2024) Heavy metals pollution from smelting activities: a threat to soil and groundwater. Ecotox Environ Safe 274:116189. https://doi.org/10.1016/j.ecoenv.2024.116189

Angon PB, Islam MS, Shreejana KC, Das A, Anjum N, Poudel A, Suchi SA (2024) Sources, effects and present perspectives of heavy metals contamination: soil, plants and human food chain. Heliyon 10:e28357. https://doi.org/10.1016/j.heliyon.2024.e28357

Bano A, Hussain J, Akbar A, Mehmood K, Anwar M, Hasni MS, Ullah S, Sajid S, Ali I (2018) Biosorption of heavy metals by obligate halophilic fungi. Chemosphere 199:218–222. https://doi.org/10.1016/j.chemosphere.2018.02.043

Bogusz A, Oleszczuk P (2020) Effect of biochar addition to sewage sludge on cadmium, copper and lead speciation in sewage sludge-amended soil. Chemosphere 239:124719. https://doi.org/10.1016/j.chemosphere.2019.124719

Bossio DA, Scow KM (1998) Impacts of carbon and flooding on soil microbial communities: phospholipid fatty acid profiles and substrate utilization patterns. Microb Ecol 35:265–278. https://doi.org/10.1007/s002489900082

Cao W, Xu H, Zhang X, Xiang W, Qi G, Wan L, Gao B (2023) Novel post-treatment of ultrasound assisting with acid washing enhance lignin-based biochar for CO2 capture: adsorption performance and mechanism. Chem Eng J 471:144523. https://doi.org/10.1016/j.cej.2023.144523

Cheah JH, Roldan JL, Ciavolino E, Ting H, Ramayah T (2021) Sampling weight adjustments in partial least squares structural equation modeling: guidelines and illustrations. Total Qual Manag Bus Excell 32:1594–1613. https://doi.org/10.1080/14783363.2020.1754125

Chen Y, Chen Q, Zhao H, Dang J, Jin R, Zhao W, Li Y (2020) Wheat straws and corn straws as adsorbents for the removal of Cr(VI) and Cr(III) from aqueous solution: kinetics, isotherm, and mechanism. ACS Omega 5:6003–6009. https://doi.org/10.1021/acsomega.9b04356

Chen R, Gao T, Cheng N, Ding G, Wang Q, Shi R, Hu G, Cai X (2021) Application of DGT/DIFS to assess bioavailable Cd to maize and its release in agricultural soils. J Hazard Mater 411:124837. https://doi.org/10.1016/j.jhazmat.2020.124837

Chen L, Han L, Sun K, Chen G, Ma C, Zhang B, Cao Y, Xing B, Yang Z (2022) Molecular transformation of dissolved organic carbon of rhizosphere soil induced by flooding and copper pollution. Geoderma 407:115563. https://doi.org/10.1016/j.geoderma.2021.115563

Chen R, Mu X, Liu J, Cheng N, Shi R, Hu M, Chen Z, Wang H (2023a) Predictive and estimation model of Cd, Ni, and Zn bioaccumulations in maize based on diffusive gradients in thin films. Sci Total Environ 860:160523. https://doi.org/10.1016/j.scitotenv.2022.160523

Chen Y, Du Z, Weng Z, Sun K, Zhang Y, Liu Q, Yang Y, Li Y, Wang Z, Luo Y, Gao B, Chen B, Pan Z, Van Zwieten L (2023b) Formation of soil organic carbon pool is regulated by the structure of dissolved organic matter and microbial carbon pump efficacy: A decadal study comparing different carbon management strategies. Glob Change Biol 29:5445–5459. https://doi.org/10.1111/gcb.16865

Chen H, Gao B, Guo Y, Yu Q, Hu M, Zhang X (2024a) Adding carbon sources to the substrates enhances Cr and Ni removal and mitigates greenhouse gas emissions in constructed wetlands. Environ Res 252:118940. https://doi.org/10.1016/j.envres.2024.118940

Chen Y, Sun K, Yang Y, Gao B, Zheng H (2024b) Effects of biochar on the accumulation of necromass-derived carbon, the physical protection and microbial mineralization of soil organic carbon. Crit Rev Environ Sci Technol 54:39–67. https://doi.org/10.1080/10643389.2023.2221155

Chen Y, Wang Z, Zhang A, Li Y, Sun K, Jiang C, Gunina A, Aloufi AS, Liang X, Han Z, Xiao Y, Zhang Y, Du Z, Zhu S, Kuzyakov Y (2025a) Polyethylene microplastics hamper aged biochar's potential in mitigating greenhouse gas emissions. Carbon Res 4:5. https://doi.org/10.1007/s44246-024-00170-9

Chen Y, Kuzyakov Y, Ma Q, Du Z, Sun K, Xiao K, Liang X, Li Y, Zhang Y, Lai X, Fu W, Gao B, Wang F, Zhu S, Gao Q, Rillig MC (2025b) Aggregate size mediates the stability and temperature sensitivity of soil organic carbon in response to decadal biochar and straw amendments. Soil Biol Biochem 211:109969. https://doi.org/10.1016/j.soilbio.2025.109969

Cheng S, Meng W, Xing B, Shi C, Wang Q, Xia D, Nie Y, Yi G, Zhang C, Xia H (2023) Efficient removal of heavy metals from aqueous solutions by Mg/Fe bimetallic oxide-modified biochar: experiments and DFT investigations. J Clean Prod 403:136821. https://doi.org/10.1016/j.jclepro.2023.136821

Cui H, Ou Y, Wang L, Yan B, Li Y, Ding D (2021) Phosphate rock reduces the bioavailability of heavy metals by influencing the bacterial communities during aerobic composting. J Integr Agric 20:1137–1146. https://doi.org/10.1016/S2095-3119(20)63300-7

Dai S, Li H, Yang Z, Dai M, Dong X, Ge X, Sun M, Shi L (2018) Effects of biochar amendments on speciation and bioavailability of heavy metals in coal-mine-contaminated soil. Hum Ecol Risk Assess 24:1887–1900. https://doi.org/10.1080/10807039.2018.1429250

Ding S, Wang Y, Zhang L, Xu L, Gong M, Zhang C (2016) New holder configurations for use in the diffusive gradients in thin films (DGT) technique. RSC Adv 6:88143–88156. https://doi.org/10.1039/c6ra19677b

Dong M, Jiang M, He L, Zhang Z, Gustave W, Vithanage M, Niazi NK, Chen B, Zhang X, Wang H, He F (2025) Challenges in safe environmental applications of biochar: identifying risks and unintended consequence. Biochar 7:12. https://doi.org/10.1007/s42773-024-00412-4

Egli M, Sartori G, Mirabella A, Giaccai D, Favilli F, Scherrer D, Krebs R, Delbos E (2010) The influence of weathering and organic matter on heavy metals lability in silicatic, Alpine soils. Sci Total Environ 408:931–946. https://doi.org/10.1016/j.scitotenv.2009.10.005

El-Naggar A, Shaheen SM, Chang SX, Hou D, Ok YS, Rinklebe J (2021) Biochar surface functionality plays a vital role in (Im)mobilization and phytoavailability of soil vanadium. ACS Sustain Chem Eng 9:6864–6874. https://doi.org/10.1021/acssuschemeng.1c01656

Fan C, Zhang Y, Wang J (2015) Influence mechanism of dissolved organic matter (DOM) from straw humification on chemical speciation of lead in loess region. Spectrosc Spectr Anal 35:3146–3150. https://doi.org/10.3964/j.issn.1000-0593(2015)11-3146-05

Fan D, Xu S, Zhu L, Zhang T, Shen D (2024) Enhancing dewaterability and reducing heavy metal leaching in industrial landfill sludge: the role of extracellular polymeric substances. Int J Environ Sci Technol. https://doi.org/10.1007/s13762-024-06043-3

Fu T, Zhang B, Gao X, Cui S, Guan C, Zhang Y, Zhang B, Peng Y (2023) Recent progresses, challenges, and opportunities of carbon-based materials applied in heavy metal polluted soil remediation. Sci Total Environ 856:158810. https://doi.org/10.1016/j.scitotenv.2022.158810

Gao B, Gao L, Zhou Y, Xu D, Zhao X (2017) Evaluation of the dynamic mobilization of vanadium in tributary sediments of the Three Gorges Reservoir after water impoundment. J Hydrol 551:92–99. https://doi.org/10.1016/j.jhydrol.2017.05.034

Gao L, Sun K, Xu D, Gao B (2020) Kinetic process of Cr(III) in contaminated soils characterized by diffusive gradients in thin films technique. Sci Total Environ 720:137425. https://doi.org/10.1016/j.scitotenv.2020.137425

Gao S, Dong Y, Jia Q, Wu S, Bai J, Cui C, Li Y, Zou P, An M, Du X, Liu H (2024) Hazards of toxic metal(loid)s: exploring the ecological and health risk in soil-crops systems with long-term sewage sludge application. Sci Total Environ 948:174988. https://doi.org/10.1016/j.scitotenv.2024.174988

Gjoka F, Felix-Henningsen P, Wegener H-R, Salillari I, Beqiraj A (2011) Heavy metals in soils from Tirana (Albania). Environ Monit Assess 172:517–527

Gryganskyi AP, Humber RA, Smith ME, Miadlikovska J, Wu S, Voigt K, Walther G, Anishchenko IM, Vilgalys R (2012) Molecular phylogeny of the Entomophthoromycota. Mol Phylogenet Evol 65:682–694. https://doi.org/10.1016/j.ympev.2012.07.026

Gul S, Whalen JK, Thomas BW, Sachdeva V, Deng H (2015) Physico-chemical properties and microbial responses in biochar-amended soils: mechanisms and future directions. Agric Ecosyst Environ 206:46–59. https://doi.org/10.1016/j.agee.2015.03.015

Haghighizadeh A, Rajabi O, Nezarat A, Hajyani Z, Haghmohammadi M, Hedayatikhah S, Asl SD, Beni AA (2024) Comprehensive analysis of heavy metal soil contamination in mining environments: impacts, monitoring techniques, and remediation strategies. Arab J Chem 17:105777. https://doi.org/10.1016/j.arabjc.2024.105777

He J, Wang S, Liu Y, Ma H, Liu Q (2017) Examining the relationship between urbanization and the eco-environment using a coupling analysis: Case study of Shanghai, China. Ecol Indic 77:185–193. https://doi.org/10.1016/j.ecolind.2017.01.017

Hurdeal VG, Gentekaki E, Hyde KD, Jeewon R (2021) Where are the basal fungi? Current status on diversity, ecology, evolution, and taxonomy. Biologia 76:421–440. https://doi.org/10.2478/s11756-020-00642-4

Irawati W, Djojo ES, Kusumawati L, Yuwono T, Pinontoan R (2021) Optimizing bioremediation: elucidating copper accumulation mechanisms of *Acinetobacter* sp. IrC2 isolated from an industrial waste treatment center. Front Microbiol 12:713812. https://doi.org/10.3389/fmicb.2021.713812

Jaremko D, Kalembasa D (2014) A comparison of methods for the determination of cation exchange capacity of soils. Ecol Chem Eng S- 21:487–498. https://doi.org/10.2478/eces-2014-0036

Ji M, Wang X, Usman M, Liu F, Dan Y, Zhou L, Campanaro S, Luo G, Sang W (2022) Effects of different feedstocks-based biochar on soil remediation: a review. Environ Pollut 294:118655. https://doi.org/10.1016/j.envpol.2021.118655

Jiang Y, Qian H, Wang X, Chen L, Liu M, Li H, Sun B (2018) Nematodes and microbial community affect the sizes and turnover rates of organic carbon pools in soil aggregates. Soil Biol Biochem 119:22–31. https://doi.org/10.1016/j.soilbio.2018.01.001

Lalonde K, Mucci A, Ouellet A, Gelinas Y (2012) Preservation of organic matter in sediments promoted by iron. Nature 483:198–200. https://doi.org/10.1038/nature10855

Li M, Cheng X, Guo H (2013) Heavy metal removal by biomineralization of urease producing bacteria isolated from soil. Int Biodeterior Biodegrad 76:81–85. https://doi.org/10.1016/j.ibiod.2012.06.016

Li Y, Gong X, Xiong J, Sun Y, Shu Y, Niu D, Lin Y, Wu L, Zhang R (2021) Different dissolved organic matters regulate the bioavailability of heavy metals and rhizosphere microbial activity in a plant-wetland soil system. J Environ Chem Eng 9:106823. https://doi.org/10.1016/j.jece.2021.106823

Li H, Yao J, Min N, Liu J, Chen Z, Zhu X, Zhao C, Pang W, Li M, Cao Y, Liu B, Duran R (2022) Relationships between microbial activity, enzyme activities and metal(loid) form in NiCu tailings area. Sci Total Environ 812:152326. https://doi.org/10.1016/j.scitotenv.2021.152326

Li A, Li A, Luo C, Liu B (2024) Assessing heavy metal contamination in *Amomum villosum* Lour. fruits from plantations in Southern China: soil-fungi-plant interactions. Ecotoxicol Environ Saf 269:115789. https://doi.org/10.1016/j.ecoenv.2023.115789

Li F, Wang H, Yang H, Xu X, Ding T, Wang Q (2025) Control of heavy metal pollution with rice husk biochar in sewage sludge compost amended soil. J Soil Sci Plant Nutr. https://doi.org/10.1007/s42729-025-02298-y

Liang Y, Han Z, Zeng Q, Wang S, Sun W, Zhong H, He Z (2022) Effective removal of Pb²⁺ from aqueous solution using magnetic mesoporous silica prepared by rubidium-containing biotite leaching residues and wastewater. Water 14:2652. https://doi.org/10.3390/w14172652

Liengaard BD (2024) Measurement invariance testing in partial least squares structural equation modeling. J Bus Res 177:114581. https://doi.org/10.1016/j.jbusres.2024.114581

Lin Y, Ye Y, Hu Y, Shi H (2019) The variation in microbial community structure under different heavy metal contamination levels in paddy soils. Ecotoxicol Environ Saf 180:557–564. https://doi.org/10.1016/j.ecoenv.2019.05.057

Liu B, Pan S, Liu Z, Li X, Zhang X, Xu Y, Sun Y, Yu Y, Zheng H (2020) Efficient removal of Cu(II) organic complexes by polymer-supported, nanosized, and hydrated Fe(III) oxides through a Fenton-like process. J Hazard Mater 386:121969. https://doi.org/10.1016/j.jhazmat.2019.121969

Liu B, Jiang S, Guan D, Song X, Li Y, Zhou S, Wang B, Gao B (2023a) Geochemical fractionation, bioaccessibility and ecological risk of metallic elements in the weathering profiles of typical skarn-type copper tailings from Tongling, China. Sci Total Environ 894:164859. https://doi.org/10.1016/j.scitotenv.2023.164859

Liu N, Li G, Su Y, Zhao Y, Ma J, Huang G (2023b) Environmental drivers and interaction mechanisms of heavy metal and antibiotic resistome exposed to amoxicillin during aerobic composting. Front Microbiol 13:1079114. https://doi.org/10.3389/fmicb.2022.1079114

Liu H, Rong X, Zhao H, Xia R, Li M, Wang H, Cui H, Wang X, Zhou J (2024) Bioaccumulation of atmospherically deposited cadmium in soybean: three-year field experiment combined with cadmium isotopes. Environ Sci Technol 58:17703–17716. https://doi.org/10.1021/acs.est.4c07961

Lu Y, Zhang Y, Cao X, Wang C, Wang Y, Zhang M, Ferrier RC, Jenkins A, Yuan J, Bailey MJ, Chen D, Tian H, Li H, von Weizsäcker EU, Zhang Z (2019) Forty years of reform and opening up: China's progress toward a sustainable path. Sci Adv 5:eaau9413. https://doi.org/10.1126/sciadv.aau9413

Ma X, Zuo H, Tian M, Zhang L, Meng J, Zhou X, Min N, Chang X, Liu Y (2016) Assessment of heavy metals contamination in sediments from three adjacent regions of the Yellow River using metal chemical fractions and multivariate analysis techniques. Chemosphere 144:264–272. https://doi.org/10.1016/j.chemosphere.2015.08.026

Ma X, Zheng C, Li W, Ai S, Zhang Z, Zhou X, Pang C, Chen H, Zhou K, Tang M, Li L, Wang Y, Li Y, Guo L, Dong H, Yang D (2017) Potential use of cotton for remediating heavy metal-polluted soils in southern China. J Soils Sediments 17:2866–2872

Meng J, Tao M, Wang L, Liu X, Xu J (2018) Changes in heavy metal bioavailability and speciation from a Pb-Zn mining soil amended with biochars from co-pyrolysis of rice straw and swine manure. Sci Total Environ 633:300–307. https://doi.org/10.1016/j.scitotenv.2018.03.199

Monecke A, Leisch F (2012) semPLS: Structural equation modeling using partial least squares. J Stat Softw 48:1–32. https://doi.org/10.18637/jss.v048.i03

Mukherjee A, Lal R (2014) Comparison of soil quality index using three methods. PLoS ONE 9:e105981. https://doi.org/10.1371/journal.pone.0105981

Naznin M, Choi J, Shin WS, Choi J (2017) Removal of metal ions from electrochemical decontamination solution using organic acids. Sep Sci Technol 52:2886–2896. https://doi.org/10.1080/01496395.2017.1375955

Nkoh JN, Ajibade FO, Atakpa EO, Abdulaha-Al Baquy M, Mia S, Odii EC, Xu R (2022) Reduction of heavy metal uptake from polluted soils and associated health risks through biochar amendment: a critical synthesis. J Hazard Mater Adv 6:100086. https://doi.org/10.1016/j.hazadv.2022.100086

Obade VdeP, Lal R (2016) Towards a standard technique for soil quality assessment. Geoderma 265:96–102. https://doi.org/10.1016/j.geoderma.2015.11.023

Pan J, Yu L (2011) Effects of Cd or/and Pb on soil enzyme activities and microbial community structure. Ecol Eng 37:1889–1894. https://doi.org/10.1016/j.ecoleng.2011.07.002

Paz-Ferreiro J, Gasco G, Gutierrez B, Mendez A (2012) Soil biochemical activities and the geometric mean of enzyme activities after application of sewage sludge and sewage sludge biochar to soil. Biol Fertil Soils 48:511–517. https://doi.org/10.1007/s00374-011-0644-3

Pueyo M, Mateu J, Rigol A, Vidal M, López-Sánchez JF, Rauret G (2008) Use of the modified BCR three-step sequential extraction procedure for the study of trace element dynamics in contaminated soils. Environ Pollut 152:330–341. https://doi.org/10.1016/j.envpol.2007.06.020

Qin S, Chen L, Fang K, Zhang Q, Wang J, Liu F, Yu J, Yang Y (2019) Temperature sensitivity of SOM decomposition governed by aggregate protection and microbial communities. Sci Adv 5:eaau1218. https://doi.org/10.1126/sciadv.aau1218

Qin G, Niu Z, Yu J, Li Z, Ma J, Xiang P (2021a) Soil heavy metal pollution and food safety in China: effects, sources and removing technology. Chemosphere 267:129205. https://doi.org/10.1016/j.chemosphere.2020.129205

Qin S, Kou D, Mao C, Chen Y, Chen L, Yang Y (2021b) Temperature sensitivity of permafrost carbon release mediated by mineral and microbial properties. Sci Adv 7:eabe3596. https://doi.org/10.1126/sciadv.abe3596

Qiu B, Tao X, Wang H, Li W, Ding X, Chu H (2021) Biochar as a low-cost adsorbent for aqueous heavy metal removal: a review. J Anal Appl Pyrolysis 155:105081. https://doi.org/10.1016/j.jaap.2021.105081

Rauret G, López-Sánchez JF, Lück D, Yli-Halla M, Muntau H, Quevauviller Ph (2001) The certification of the extractable contents (mass Fractions) of Cd, Cr, Cu, Ni, Pb and Zn in freshwater sediment following a sequential extraction procedure BCR-701. Directorate-General for Research.

Rehman M, Liu L, Bashir S, Saleem MH, Chen C, Peng D, Siddique KHM (2019) Influence of rice straw biochar on growth, antioxidant capacity and copper uptake in ramie (*Boehmeria nivea* L.) grown as forage in aged copper-contaminated soil. Plant Physiol Biochem 138:121–129. https://doi.org/10.1016/j.plaphy.2019.02.021

Rizwan MS, Imtiaz M, Zhu J, Yousaf B, Hussain M, Ali L, Ditta A, Ihsan MZ, Huang G, Ashraf M, Hu H (2021) Immobilization of Pb and Cu by organic and inorganic amendments in contaminated soil. Geoderma 385:114803. https://doi.org/10.1016/j.geoderma.2020.114803

Shen Y, Tong Q, Li Y, Shi J, Zhang X, Shao Y, Li Y (2022) Effect of straw pretreatment on Cu and Zn passivation and dissolved organic matter in mixed anaerobic fermentation of straw and pig manure. Bioenerg Res 15:1626–1638. https://doi.org/10.1007/s12155-021-10381-2

Shentu J, Li X, Han R, Chen Q, Shen D, Qi S (2022) Effect of site hydrological conditions and soil aggregate sizes on the stabilization of heavy metals (Cu, Ni, Pb, Zn) by biochar. Sci Total Environ 802:149949. https://doi.org/10.1016/j.scitotenv.2021.149949

Siedt M, Schaeffer A, Smith KEC, Nabel M, Ross-Nickoll M, van Dongen JT (2021) Comparing straw, compost, and biochar regarding their suitability as agricultural soil amendments to affect soil structure, nutrient leaching, microbial communities, and the fate of pesticides. Sci Total Environ 751:141607. https://doi.org/10.1016/j.scitotenv.2020.141607

Song P, Xu D, Yue J, Ma Y, Dong S, Feng J (2022) Recent advances in soil remediation technology for heavy metal contaminated sites: a critical review. Sci Total Environ 838:156417. https://doi.org/10.1016/j.scitotenv.2022.156417

Sun F, Xu Z, Fan L (2021) Response of heavy metal and antibiotic resistance genes and related microorganisms to different heavy metals in activated sludge. J Environ Manage 300:113754. https://doi.org/10.1016/j.jenvman.2021.113754

Sungur A, Soylak M, Ozcan H (2014) Investigation of heavy metal mobility and availability by the BCR sequential extraction procedure: relationship between soil properties and heavy metals availability. Chem Speciation Bioavailab 26:219–230. https://doi.org/10.3184/095422914X14147781158674

Tian K, Xing Z, Liu G, Wang H, Jia M, Hu W, Huang B (2018) Cadmium phytoavailability under greenhouse vegetable production system measured by diffusive gradients in thin films (DGT) and its implications for the soil threshold. Environ Pollut 241:412–421. https://doi.org/10.1016/j.envpol.2018.05.086

Tian L, Fu K, Chen S, Yao J, Bian L (2022) Comparison of microscopic adsorption characteristics of Zn(II), Pb(II), and Cu(II) on kaolinite. Sci Rep. https://doi.org/10.1038/s41598-022-20238-z

Tuan MN, Seo C, Ji M, Paik M-J, Myung S-W, Kim J (2018) Effective soil extraction method for cultivating previously uncultured soil bacteria. Appl Environ Microbiol 84:e01145-e1218. https://doi.org/10.1128/AEM.01145-18

Tuo P, Zhang Z, Du P, Hu L, Li R, Ren J (2024) Changes in coal waste DOM chemodiversity and Fe/Al oxides during weathering drive the fraction conversion of heavy metals. Sci Total Environ 926:172063. https://doi.org/10.1016/j.scitotenv.2024.172063

Upadhyay SK, Kumar P, Jain D, Zhao X (2025) Convergence of nanotechnology and microbial-electrochemical systems for next-generation of toxic heavy metal and organic pollutant soil removal. J Environ Chem Eng 13:118272. https://doi.org/10.1016/j.jece.2025.118272

Wang J, Pan F, Soininen J, Heino J, Shen J (2016) Nutrient enrichment modifies temperature-biodiversity relationships in large-scale field experiments. Nat Commun 7:13960. https://doi.org/10.1038/ncomms13960

Wang J, Song Y, Ma T, Raza W, Li J, Howland JG, Huang Q, Shen Q (2017a) Impacts of inorganic and organic fertilization treatments on bacterial and fungal communities in a paddy soil. Appl Soil Ecol 112:42–50. https://doi.org/10.1016/j.apsoil.2017.01.005

Wang N, Xue X, Juhasz AL, Chang Z, Li H (2017b) Biochar increases arsenic release from an anaerobic paddy soil due to enhanced microbial reduction of iron and arsenic. Environ Pollut 220:514–522. https://doi.org/10.1016/j.envpol.2016.09.095

Wang J, Chen R, Fan L, Cui L, Zhang Y, Cheng J, Wu X, Zeng W, Tian Q, Shen L (2021a) Construction of fungi-microalgae symbiotic system and adsorption study of heavy metal ions. Sep Purif Technol 268:118689. https://doi.org/10.1016/j.seppur.2021.118689

Wang M, Zhao S, Wang L, Chen S, Li S, Lei X, Sun X, Qin L (2021b) Salt stress-induced changes in microbial community structures and metabolic processes result in increased soil cadmium availability. Sci Total Environ 782:147125. https://doi.org/10.1016/j.scitotenv.2021.147125

Wang L, Chen D, Zhu L (2023) Biochar carbon sequestration potential rectification in soils: Synthesis effects of biochar on soil CO2, CH4 and N2O emissions. Sci Total Environ 904:167047. https://doi.org/10.1016/j.scitotenv.2023.167047

Wang H, Zhang H, He L, Wang J, Wang S, Shi X, Zhang X, Wang H, He F (2025) Environmental behavior of per- and polyfluoroalkyl substances (PFASs) and the potential role of biochar for its remediation: a review. Biochar 7:14. https://doi.org/10.1007/s42773-024-00410-6

Wei T, Gao H, An F, Ma X, Hua L, Guo J (2023a) Performance of heavy metal-immobilizing bacteria combined with biochar on remediation of cadmium and lead co-contaminated soil. Environ Geochem Health 45:6009–6026. https://doi.org/10.1007/s10653-023-01605-9

Wei W, Ling S, Wu X, Li X (2023b) Geochemical accumulation and source tracing of heavy metals in arable soils from a black shale catchment, southwestern China. Sci Total Environ 857:159467. https://doi.org/10.1016/j.scitotenv.2022.159467

Weng Z, Van Zwieten L, Singh BP, Tavakkoli E, Kimber S, Morris S, Macdonald LM, Cowie A (2018) The accumulation of rhizodeposits in organo-mineral fractions promoted biochar-induced negative priming of native soil organic carbon in Ferralsol. Soil Biol Biochem 118:91–96. https://doi.org/10.1016/j.soilbio.2017.12.008

Weng C, Jia S, Wang D, Ma W (2024) Pollution characteristics of heavy metal(loid)s in soil in China: implications for health risk assessment and temporal trend analysis. Environ Chem Ecotoxicol 6:248–258. https://doi.org/10.1016/j.enceco.2024.07.007

Wu S, Li H, Zhang D, Zhang H (2023) Simultaneous determination of heavy metal concentrations and toxicities by diffusive gradient in thin films containing *Acinetobacter* whole-cell bioreporters (Bio-DGT). Environ Pollut 320:121050. https://doi.org/10.1016/j.envpol.2023.121050

Xie Y, Bu H, Feng Q, Wassie M, Amee M, Jiang Y, Bi Y, Hu L, Chen L (2021) Identification of Cd-resistant microorganisms from heavy metal-contaminated soil and its potential in promoting the growth and Cd accumulation of bermudagrass. Environ Res 200:111730. https://doi.org/10.1016/j.envres.2021.111730

Xu Q, Gao L, Peng W, Gao B, Xu D, Sun K (2018) Assessment of labile Zn in reservoir riparian soils using DGT, DIFS, and sequential extraction. Ecotox Environ Safe 160:184–190. https://doi.org/10.1016/j.ecoenv.2018.05.039

Yang Y, Gunina A, Cheng H, Liu L, Wang B, Dou Y, Wang Y, Liang C, An S, Chang S (2025) Unlocking mechanisms for soil organic matter accumulation: carbon use efficiency and microbial necromass as the keys. Glob Change Biol 31:e70033. https://doi.org/10.1111/gcb.70033

Zhang C, Nie S, Liang J, Zeng G, Wu H, Hua S, Liu J, Yuan Y, Xiao H, Deng L, Xiang H (2016) Effects of heavy metals and soil physicochemical properties on wetland soil microbial biomass and bacterial community structure. Sci Total Environ 557:785–790. https://doi.org/10.1016/j.scitotenv.2016.01.170

Zhang J, Li C, Li G, He Y, Yang J, Zhang J (2021) Effects of biochar on heavy metal bioavailability and uptake by tobacco (*Nicotiana tabacum*) in two soils. Agric Ecosyst Environ 317:107453. https://doi.org/10.1016/j.agee.2021.107453

Zhang R, Liu Z, Wang Y, Jiang Z, Li M, Li H, Zhao X, Duan Z, Song X (2025) Effects of intercropping on composition and molecular diversity of soil dissolved organic matter in apple orchards: different roles of bacteria and fungi. Agric Ecosyst Environ 382:109509. https://doi.org/10.1016/j.agee.2025.109509

Zhong X, Yang Y, Liu H, Fang X, Zhang Y, Cui Z, Lv J (2023) New insights into the sustainable use of soluble straw humic substances for the remediation of multiple heavy metals in contaminated soil. Sci Total Environ 903:166274. https://doi.org/10.1016/j.scitotenv.2023.166274

Zhou G, Eisenhauer N, Terrer C, Eldridge DJ, Duan H, Guirado E, Berdugo M, Zhou L, Liu S, Zhou X, Delgado-Baquerizo M (2024) Resistance of ecosystem services to global change weakened by increasing number of environmental stressors. Nat Geosci 17:882–888. https://doi.org/10.1038/s41561-024-01518-x

Zhu Q, Wu J, Wang L, Yang G, Zhang X (2015) Effect of biochar on heavy metal speciation of paddy soil. Water Air Soil Pollut 226:429. https://doi.org/10.1007/s11270-015-2680-3

Zhu Q, Liang Y, Zhang Q, Zhang Z, Wang C, Zhai S, Li Y, Sun H (2023) Biochar derived from hydrolysis of sewage sludge influences soil properties and heavy metals distributed in the soil. J Hazard Mater 442:130053. https://doi.org/10.1016/j.jhazmat.2022.130053